



Rough set based bilateral filter design for denoising brain MR images

Ashish Phophalia, Suman K. Mitra*

Dhirubhai Ambani Institute of Information and Communication Technology, Gandhinagar, India



ARTICLE INFO

Article history:

Received 10 June 2014

Received in revised form 2 April 2015

Accepted 3 April 2015

Available online 21 April 2015

Keywords:

Image denoising

Magnetic resonance imaging (MRI)

Rough set theory (RST)

ABSTRACT

A study on bilateral filter for denoising reveals that more informative the filters are, better is the result expected. Moreover, getting precise information of the image with noise is a difficult task. In the current work, a rough set theory (RST) based approach is used to derive pixel level edge map and class labels which in turn are used to improve the performance of bilateral filters. RST handles the uncertainty present in the data even under noise. The basic structure of existing bilateral filter is not changed much, however, boosted up by prior information derived by rough edge map and rough class labels. The filter is extensively applied to denoise brain MR images. The results are compared with that of the state-of-the-art approaches. The experiments have been performed on two real (normal and pathological disordered) human MR databases. The performance of the proposed filter is found to be better, in terms of benchmark metrics.

© 2015 Elsevier B.V. All rights reserved.

1. Introduction

Denoising is one of the initial preprocessing tasks for medical image analysis. The acquisition process of medical images is highly sensitive to noise or undesired signals. In general, the noise realization is assumed to be Gaussian in nature. However, it has been shown that the noise in Magnetic Resonance (MR) Image could be Rician in nature [1]. But assumption of having Gaussian noise in place of Rician noise in low Signal to Noise Ratio (SNR) MRI is still holds good. Be it Gaussian or Rician, removal of noise from MR images is essential for further analysis.

Initial work in the domain of denoising includes Mean and Median filters, Isotropic filter, anisotropic filter [2–4], robust statistics [5] and [6]. Furthermore, non-iterative and more edge preserving Bilateral Filter (BF) proposed in [7], revolutionized the notion of denoising. The origin of BF has been shown from Anisotropic diffusion methods under Bayesian approach in [8]. BF uses two components, one on spatial location and another on intensity values simultaneously. Since its inception, there have been many modifications of Bilateral Filter as suggested in [9–13]. However, its constant time version, in terms of computational complexity, has been proposed recently in [14,15]. It is even extended to

Trilateral filters [16,17]. The third component which is used simultaneously with existing two in BF, is designed in various ways. It seems that more information could lead to better performance. In the present article, the filter proposed is trilateral by nature. The third component of the filter is based on edge information and neighborhood information. Various edge detectors, such as Canny method [18] or segmentation methods and gradient based methods such as Active Contour Methods [19,20], could be utilized for obtaining edge details. However, we are looking for edges that give rise to object boundaries which are closed in nature. Most of the above mentioned methods fail to get such closed boundaries while finding the edges. Moreover, the method such as Active Contour fails to get object boundaries where number of objects is not in power of two. The current work is based on rough set theory (RST), [21], to find object boundaries which are closed and continuous. As mentioned previously, the third component of filter also depends on neighborhood information, each image pixel is labeled as one of the objects/classes present in the image. This class information (class label) is obtained through the Rough set based mechanism. In fact, the edge map and class labels are obtained simultaneously. There are few methods available which use pair of images to denoise under bilateral framework, such as cross bilateral filter and dual bilateral filter (readers are suggested to refer [22] for more details).

A rough set based rough edge map (REM) and rough class label (RCL) are used along with spatial and intensity information as mentioned in bilateral filter. REM strongly controls the effect of Bilateral Filter on edge and non-edge pixels whereas the RCL keeps track of the homogeneity within object and heterogeneity on the edges.

* Corresponding author at: DA-IICT, Post Bag 4, Near Indroda Circle, Gandhinagar 382007, Gujarat, India. Tel.: +91 79 30510584; fax: +91 79 30520010.

E-mail addresses: ashish.phophalia@daiict.ac.in (A. Phophalia), suman.mittra@daiict.ac.in (S.K. Mitra).

URL: <http://intranet.daiict.ac.in/suman.mittra/newSite/> (S.K. Mitra).

The proposed filter serves as a joint framework for image segmentation and denoising problem, which the conventional Bilateral Filter lacks. The filter has been applied to a large set of images with various image quality measures like peak signal to noise (PSNR) ratio, root mean squared error (RMSE), Structural Similarity Index (SSIM) in [23] and Feature Similarity Index (FSIM) in [24]. The performance of proposed filter is found to be comparable with the conventional methods of denoising using existing Bilateral and trilateral filters in the light of above measures. Note that progress has been made in image denoising using methods based on non-locality [25] and its implementation in medical images ([26–28]). Research is still continuing based on Non-local principle ([29–33]). Main motivation of the present work is to examine the compatibility of RST to obtain edge and neighborhood information that could be utilized in designing a trilateral filter for medical image denoising (MID) problem. Hence, the method is compared with methods under the bilateral framework only. However, this is an extension of our previous work [34] with an exhaustive set of experiments and results. The proposed method has been applied on wide range of noise level and different modalities of phantom MR images. We have presented results on human brain MR images with pathological disorder also.

The paper is organized as follows: bilateral filter and its variants are presented in Section 2 for sake of completeness. Section 3 presents the proposed approach for MR image denoising problem, Section 4 presents experimental results on human brain MR images with visual examples and comparison with some of the state-of-the-art algorithms. Section 5 concludes the manuscript.

2. Related work

The bilateral filter (BF) inherently defines spatial and range (photometric) filter to denoise an image according to spatial domain and intensity domain respectively [7]. The final filter uses the product of weights of both the filters for a neighboring pixel. Mathematically, BF can be defined as

$$\Delta(i, j) = \psi(i, j)\zeta(i, j) \quad (1)$$

where ψ and ζ are monotonically decreasing non-negative functions for spatial and intensity closeness, i is the center pixel location and location j is in neighborhood of i , i.e. $j \in N(i)$, within window $w \times w$. In general, both functions are assumed to be Gaussian in nature and controlled by their parameters, σ_ψ and σ_ζ respectively. These functions are defined as

$$\psi(i, j) = G_{\sigma_\psi}(\|i - j\|) \quad (2)$$

$$\zeta(i, j) = G_{\sigma_\zeta}(\|Y(i) - Y(j)\|) \quad (3)$$

where $Y(i)$ represent intensity at location i . The denoised pixel intensity $\hat{Y}(i)$ at the location i is given by

$$\hat{Y}(i) = \frac{\sum_{j \in N(i)} \Delta(i, j) Y(j)}{\sum_{j \in N(i)} \Delta(i, j)} \quad (4)$$

The scaled bilateral filter proposed in [10], is one of state-of-the-art approach proposed on conventional BF framework. The key idea behind this is consider the closeness in the scale-space domain where noise will get suppressed by some amount. In this approach, input is first convolved with a Gaussian kernel of suitable size. In its intensity filter, the difference is considered between scaled version of input image at location p with input image at location q . But this blurring may lead to a loss of edge information. The selection of appropriate scale for comparison purpose was not suggested. The spatial filter is kept same. The intensity filter, ζ , is defined as follows:

$$\zeta(p, q) = G_{\sigma_\zeta}(\|I_G(p) - I(q)\|) \quad (5)$$

$$I_G(p) = \sum_{q \in N(p)} G_{scale}(\|p - q\|) I(q) \quad (6)$$

Here, I_G is the scaled version of input image I , p and q are positions in the image and $N(p)$ is the neighborhood considered around position p .

A Wavelet based bilateral filter has been proposed in [13] in multi-resolution framework. An input image is decomposed into its approximation (LL band) and detail sub-bands (LH, HL, HH bands) through wavelet decomposition at two levels using 'db8' filter. The BF is applied on approximation sub-band at both level and wavelet thresholding is applied on detail sub-bands. The denoised image is reconstructed using filtered approximation band and detail sub-bands (after applying thresholding on coefficients) at both the level using inverse wavelet transformation. The structure and behavior of conventional Bilateral Filter [7] remains intact (refer to Eq. (1)), however, it is applied at various level of wavelet pyramid structure. More details can be found in [13].

In BF, a pixel is estimated using weighted average of pixels in the given neighborhood space as discussed above. The extreme case of it can be defined if the neighborhood window is assumed to be equal to given image space for each pixel. This philosophy leads to the concept of non local means [25] approach designed for image denoising. Non-Local similarity focuses on the range filter by leveraging the effect of spatial filter in predefined neighborhood. In other words, it inherently assumes complete image space and estimation is based on weighted average of range kernel function. However, for computationally efficient process, a sufficiently large window is considered around each pixel to search for similar pixels in terms of intensity. The non local means is often considered as a generalization of bilateral filter. More details can be found in [25].

3. Proposed method

The major contribution of this work is to provide more information from noisy image in the Bilateral framework to boost up the performance. Under BF, edge information can be used to stop denoising process across the boundaries. But the presence of noise makes it more difficult to get actual edges, hence makes it an ill-posed problem as mentioned in [35]. This prompted the present work to select Rough Set Theory (RST) to get imprecise edge information that is expected to include actual edges. The granule information processing of RST helps to visualize the possible presence of edge or heterogeneity in the granules. Granules are defined as tiny image blocks of size either 2×1 , 1×2 or 2×2 etc. The RST based approach, with the help of granules, provides partitions in the image to create lower and upper approximations of the object. These are known as object lower and upper approximation set. Note that, lower approximation set will be contained in upper approximation set. The difference of both approximations provides a possible edge region for a particular object or class present in the image. Here, in this work, we considered four major class/objects namely, CSF, White matter, Gray matter and Background in the brain MR images. For denoising task, to enhance the performance of the bilateral filter, the rough edge map (REM) of the image and rough class labels (RCL) of each pixel are obtained. The procedure for obtaining REM and RCL are presented in next two sections followed by design of proposed filter.

3.1. Assignment of class labels

Objective of this step is to assign a class label to each individual pixel. However, presence of noise makes this task hard. It is even harder as noise level increases. Finding a suitable threshold from the histogram of the image is a common practice to discriminate objects and thereby assigning class label to the pixels. But,

histogram of noisy image may not lead to precise threshold for object segmentation. This imprecise threshold in turn will define imprecise object boundary that could affect the performance of Bilateral Filter. RST, being known for handling impreciseness, is expected to give rise a threshold that could boost up the performance of Bilateral Filter.

The impreciseness is avoided as far as possible by optimizing Rough Entropy to find a threshold as precise as possible. Now onwards, this threshold will be referred as Rough Entropy Threshold (RE_T). Originally, RE_T was proposed for a two class problem [35], known as binarization. Initial approximate value of a threshold (valley in the histogram) is obtained using a window based method from the histogram. This value is then refined by optimizing Rough Entropy criteria, defined as [35]:

$$RE_T = -\frac{1}{2} \left[R_{O_T} \log_e \left(\frac{R_{O_T}}{e} \right) + R_{B_T} \log_e \left(\frac{R_{B_T}}{e} \right) \right] \quad (7)$$

where $R_{O_T} = 1 - |\bar{O}_T|/|O_T|$ and $R_{B_T} = 1 - |\bar{B}_T|/|B_T|$ ($|\bar{S}|$ and $|S|$ are cardinality of lower and upper approximation of set S respectively) are roughness of object of interest (O_T) and background (B_T) respectively.

In the present context, we are using MR images (noisy) having more than two classes. The above defined RE_T for two class problem is applied in successive manner to get thresholds for multi-modal histogram. The threshold of an object is obtained by considering this current object as one class and all other objects as another class (background). The image thus binarized depicts only one object. After getting the first threshold, each pixel is assigned a single bit binary symbol 0 or 1 depending on whether it is below threshold or above threshold respectively. The procedure is repeated with

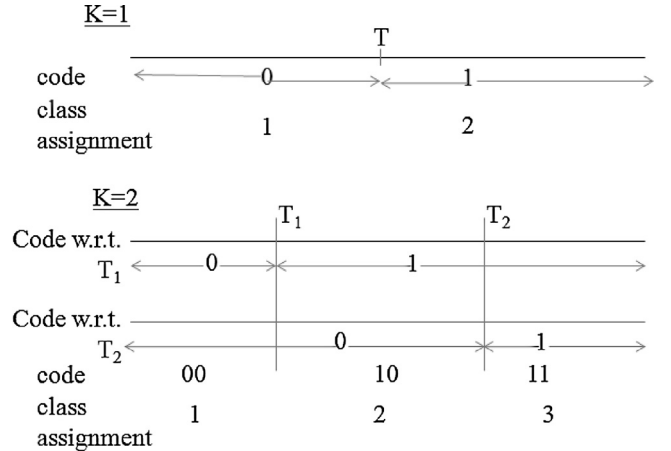


Fig. 1. Code and class assignment for different number of thresholds. Here K is number of thresholds.

respect to other objects. So in case, there are N objects, $N - 1$ thresholds are obtained and consequently at the end, each pixel will get a binary code of length $N - 1$. It is expected that, out of 2^{N-1} possible binary codes, there only N different binary codes will be assigned to all pixels. Pixels having same binary code belong to the same class. By this way, class labels are assigned to each pixel. A figurative explanation is shown in Fig. 1.

The entire procedure is summarized below

1. Estimate approximate thresholds from the noisy image histogram using parzen window approach.

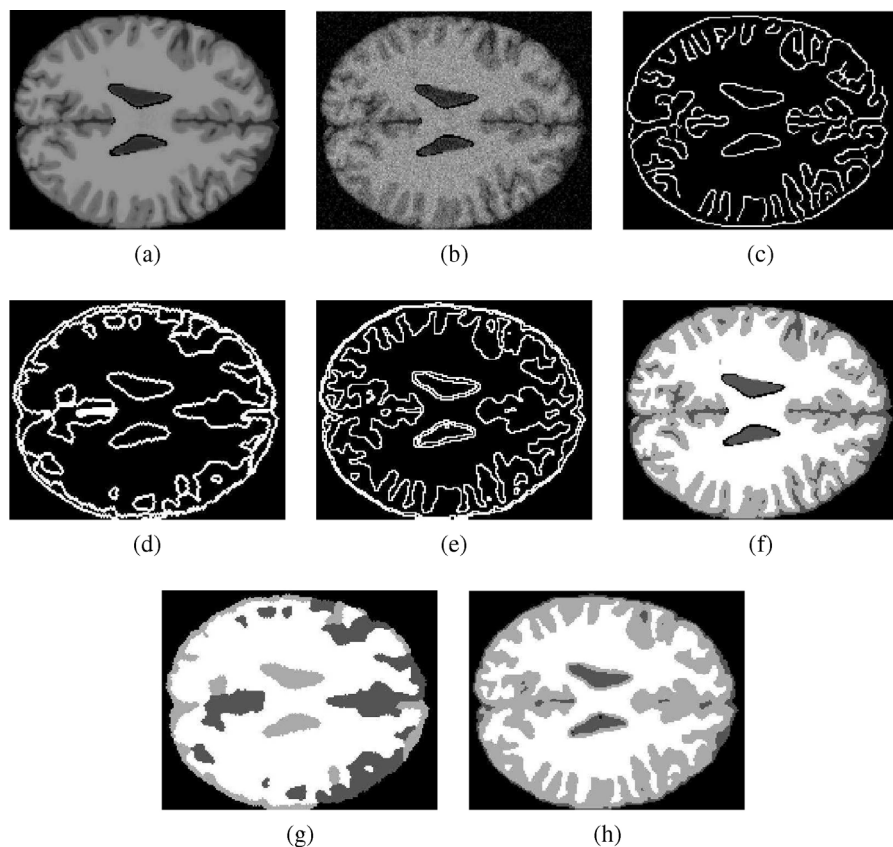


Fig. 2. (a) Noise free MR Image, (b) Noisy MR Image, (c) Canny edge detection on noisy image (d) Boundary extraction from MCV method, (e) Boundary extraction from proposed RST based method, (f) Ground Truth segmentation of noise free MR image (a), (g) Segmentation from MCV method, accuracy = 68.84% and (h) Segmentation from proposed method, accuracy = 91.87%.

Table 1

Parameter values used in this work for all the methods.

Approach	# of parameters	Parameter value
Bilateral filter [7]	2	$\sigma_\psi = 5$ and $\sigma_\zeta = 0.01$
Multi resolution	3	$\sigma_\psi = 5, L = 2$
Bilateral filter [13]		$\sigma_\zeta = \text{estimated noise level}$ at each wavelet decomposition
Scaled bilateral filter [10]	3	$\text{scale} = 0.5, \sigma_\psi = 5$ and $\sigma_\zeta = 0.01$
NLM filter [25]	3	search window size= 11×11 , $\text{patchsize} = 3 \times 3$ $h = \text{SD of noise in the image}$
Proposed filter	3	$\sigma_\psi = 5$ and $\sigma_\zeta = 0.01$ $\rho = \text{either } \rho_s, \rho_m \text{ or } \rho_l$

2. Optimize each threshold separately using rough entropy criteria (Eq. (7)).
3. Binarize the image with respect to each optimized threshold. For each threshold, assign 1 if pixel value is greater or equal to the threshold, 0 otherwise.
4. Combine assigned symbols (1 or 0) of each pixel for all thresholds. This will lead to representing each pixel by a binary string of length K , if there are K thresholds.
5. Classify all binary strings and thereby pixels. Strings having same symbol at same position will be classified as same class.

3.2. Derivation of rough edge map (REM)

The size of granules is an important factor for finding REM. For deriving edge information, a heterogeneous granule is considered as having a possible edge location. In this work, the granule size is

Table 2

Performance comparison of proposed denoising filter with other approaches on various quantitative measures under **Gaussian Noise** assumption on **T1** images of Brain Web database.

Noise	Methods	Slice 70				Slice 100			
		PSNR	RMSE	MSSIM	FSIM	PSNR	RMSE	MSSIM	FSIM
3	Noisy image	39	8.18	0.9472	0.9752	39.18	7.85	0.9345	0.973
	Bilateral	40.23	6.17	0.9644	0.9866	40.81	5.39	0.9612	0.9869
	Multi resolution bilateral	35.19	19.68	0.9275	0.9566	37.57	11.37	0.9533	0.9769
	Scaled bilateral	40.09	6.37	0.9661	0.9903	40.32	6.03	0.9637	0.9906
	Non local means	38.49	9.21	0.9731	0.9902	40.05	6.43	0.9705	0.9918
	Proposed method	40.6	5.66	0.9686	0.9898	41.35	4.75	0.9676	0.9907
5	Noisy image	34.57	22.72	0.8776	0.9409	34.75	21.8	0.8541	0.9358
	Bilateral	35.25	19.27	0.898	0.9546	35.64	17.75	0.8835	0.9522
	Multi resolution bilateral	33.04	32.28	0.8840	0.9372	34.39	23.68	0.9058	0.9610
	Scaled bilateral	35.78	17.15	0.9099	0.9683	36.14	15.81	0.9017	0.9676
	Non local means	37.21	12.35	0.9505	0.9842	38.47	9.25	0.9415	0.9867
	Proposed method	36.53	14.44	0.9293	0.9772	37.36	11.95	0.9288	0.9793
7	Noisy image	31.64	44.54	0.8028	0.9025	31.82	42.74	0.7735	0.8974
	Bilateral	32.07	40.35	0.8191	0.914	32.33	38	0.7951	0.9081
	Multi resolution bilateral	31.28	48.42	0.8391	0.9144	32.12	39.90	0.8577	0.9406
	Scaled bilateral	32.69	34.96	0.8387	0.9342	33.06	32.15	0.8243	0.9317
	Non local means	35.92	16.65	0.9272	0.9770	37.01	12.95	0.9136	0.9811
	Proposed method	33.58	28.5	0.8734	0.9547	34.2	24.72	0.8648	0.953
10	Noisy image	28.55	90.89	0.6971	0.8458	28.72	87.22	0.6679	0.8352
	Bilateral	28.77	86.34	0.7068	0.8534	28.98	82.83	0.6795	0.8439
	Multi resolution bilateral	29.3	76.41	0.7783	0.8787	29.88	66.86	0.7954	0.9086
	Scaled bilateral	29.45	73.79	0.7323	0.8779	29.74	69.08	0.712	0.8706
	Non local means	34.08	25.38	0.8949	0.9647	34.99	20.59	0.8782	0.9705
	Proposed method	31.13	50.15	0.8156	0.936	31.67	44.26	0.8171	0.9433
15	Noisy image	25.02	204.45	0.5524	0.7635	25.2	196.21	0.5323	0.7504
	Bilateral	25.13	199.67	0.5566	0.7673	25.31	191.34	0.5367	0.7545
	Multi resolution bilateral	27.19	124.24	0.7051	0.8321	27.86	106.42	0.7290	0.8709
	Scaled bilateral	25.86	168.82	0.5831	0.7927	26.09	160.05	0.5649	0.7807
	Non local means	31.48	46.16	0.8441	0.9383	32.08	40.31	0.8270	0.9455
	Proposed method	27	129.88	0.64	0.8477	27.54	114.49	0.6481	0.8612

kept as 2×2 . This leads to a situation where some granule will not be counted entirely in lower approximation of an object. All such granules will be considered as boundary for an object and union of all object boundaries will give an REM of the image [36].

The problem now turns to find those granules which are possibly on the boundary of an object. This can be done by considering each optimized threshold separately. First, binarize the image corresponding to each optimized threshold. A granule will be called *homogeneous*, if all the pixels of the granule are either below threshold or above it. Otherwise, it will be *heterogeneous* in nature, which in fact will form the edge map of the image. The resultant edge map on the Noisy MR image is shown in the Fig. 2. It includes result of Canny edge detector [18] and Multiphase Chan-Vese (MCV) Active Contour Method (Proposed in [37]) along with proposed method on noisy image. A visual comparison indicates that the REM of the image includes all edges obtained from canny. However, REM is a granule based approach that would generate single pixel edge. The segmentation map of the proposed approach also shown along with ground truth segmentation [38] and segmentation obtained from MCV method. The segmentation accuracy of proposed method is 91.87% instead of 68.84% in MCV method.

3.3. Proposed filter

The proposed filter introduces a term which boosts up the impact of spatial closeness and intensity closeness. The introduced term is adaptive in nature and derived from RCL and REM obtained from noisy image. The spatial filter in the conventional approach does not consider presence of edge in the image. Similarly, range filter is simply governed by parameters of functional form like

Table 3

Performance comparison of proposed denoising filter with other approaches on various quantitative measures under **Gaussian Noise** assumption on **T2** images of Brain Web database.

Noise SD	Methods	Slice 70				Slice 100			
		PSNR	RMSE	MSSIM	FSIM	PSNR	RMSE	MSSIM	FSIM
3	Noisy image	39	8.17	0.949	0.9793	39.18	7.85	0.9372	0.9769
	Bilateral	40.14	6.25	0.9663	0.9887	40.79	5.42	0.9638	0.9892
	Multi resolution bilateral	30.89	52.94	0.8795	0.9121	33.14	31.54	0.9330	0.9492
	Scaled bilateral	39.08	8.04	0.9682	0.9913	38.75	8.67	0.9668	0.9923
	Non local means	34.06	25.49	0.9724	0.9873	34.90	21.03	0.9698	0.9889
	Proposed method	40.5	5.79	0.9705	0.991	41.25	4.88	0.9697	0.9921
7	Noisy image	31.67	44.22	0.8124	0.92	31.85	42.5	0.7852	0.9101
	Bilateral	32.08	40.31	0.8281	0.9292	32.33	38.02	0.8059	0.9219
	Multi resolution bilateral	28.09	100.98	0.8106	0.8784	29.57	71.73	0.8503	0.9185
	Scaled bilateral	32.55	36.13	0.8492	0.947	32.8	34.15	0.8368	0.9452
	Non local means	32.65	35.35	0.9296	0.9744	33.32	30.26	0.9175	0.9786
	Proposed method	33.3	30.4	0.8705	0.9575	33.81	27.04	0.8652	0.957
10	Noisy image	28.6	89.81	0.7166	0.8745	28.76	86.48	0.6893	0.86
	Bilateral	28.82	85.33	0.7259	0.8808	29.01	81.66	0.7002	0.8675
	Multi resolution bilateral	26.47	146.58	0.7701	0.8582	27.67	111.26	0.8030	0.8969
	Scaled bilateral	29.43	74.2	0.7517	0.9028	29.68	70.02	0.7328	0.8957
	Non local means	31.47	46.26	0.8992	0.9628	31.15	39.60	0.8845	0.9676
	Proposed method	31.01	51.59	0.8411	0.9299	30.98	51.96	0.8067	0.9393
15	Noisy image	25.1	200.95	0.5917	0.8094	25.26	193.86	0.5722	0.79
	Bilateral	25.21	196.08	0.5958	0.8127	25.37	188.86	0.5765	0.7935
	Multi resolution bilateral	24.28	242.76	0.7129	0.8252	25.03	204.42	0.7356	0.8550
	Scaled bilateral	25.86	168.62	0.6203	0.8342	26.07	160.54	0.6024	0.8192
	Non local means	29.60	71.17	0.8494	0.9398	30.18	62.32	0.8371	0.9453
	Proposed method	28.48	92.25	0.7604	0.9078	28.69	87.85	0.7405	0.9057
20	Noisy image	22.62	355.37	0.5015	0.7565	22.77	343.43	0.49	0.7338
	Bilateral	22.69	350.31	0.5037	0.7584	22.84	338.31	0.4919	0.756
	Multi resolution bilateral	22.56	360.91	0.6627	0.7899	23.17	313.07	0.6843	0.8159
	Scaled bilateral	23.42	295.54	0.5264	0.7794	23.58	285.04	0.5137	0.7580
	Non local means	27.85	104.95	0.8006	0.9162	28.51	91.74	0.7938	0.9225
	Proposed method	25.59	179.47	0.6313	0.8526	25.78	171.65	0.6114	0.8393
25	Noisy image	20.71	552.55	0.4343	0.712	20.85	534.03	0.4285	0.688
	Bilateral	20.75	547.7	0.4354	0.7133	20.9	529.16	0.4296	0.6892
	Multi resolution bilateral	21.3	482.08	0.6227	0.7585	21.73	436.39	0.6415	0.7796
	Scaled bilateral	21.53	457	0.4556	0.7336	21.69	440.93	0.4481	0.7091
	Non local means	26.54	144.14	0.7553	0.8949	27.08	137.32	0.7524	0.9002
	Proposed method	22.87	335.54	0.5149	0.7876	22.88	335.4	0.4957	0.7661

decay parameter if function is assumed to be Gaussian. This leads to include more information about edges and homogeneous region of the image.

The third term $\rho(i,j) \in [0, 1]$ is defined for each pixel of the image conditioned on REM information around pixel (x, y) and RCL information at location (i, j) (Here, (x,y) is the center pixel location in the image space and (i,j) location is in the predefined neighborhood of (x,y) location). Both the information utilizes the uncertainty or roughness of the image due to presence of noise. In this proposal, a fuzzy notion is adopted to derive the value of ρ for each pixel depending on both the information. Here, the value of ρ is categorized in three notions, namely small (ρ_s), moderate (ρ_m) and high

(ρ_h) based on impact of both the information for each pixel. The restriction of ρ is defined as follows

1. $\rho_h(i,j) \in [0, 0.4]$
2. $\rho_m(i,j) \in (0.4, 0.7]$
3. $\rho_s(i,j) \in (0.7, 1]$

So far, the ranges of small, medium and large values of ρ are fixed intuitively by looking at its impact on the filter. However, a sigmoidal type of function could be used. The third weight (ρ) is expected to either boost up or lower down the effect of other two weights in conventional Bilateral Filter. Here, (x, y) represents center pixel location of window $w \times w$ and location (i, j) defines to be neighbors of (x, y) in the window. The pseudo assignment is as follows:

1. if $REM(i,j) == 1$
2. if $class(i,j) == class(x, y)$
3. $\rho(i,j) = \rho_m$;
4. else
5. $\rho(i,j) = \rho_s$;
6. end
7. else
8. if $class(i,j) == class(x, y)$
9. if $REM(x, y) == 1$

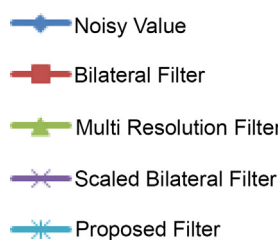


Fig. 3. Legends used for graphs in Fig. 4 and 5.

Table 4

Performance comparison of proposed denoising filter with other approaches on various quantitative measures under **Rician Noise** assumption on **T1** images of Brain Web database.

Noise SD	Methods	Slice 70				Slice 100			
		PSNR	RMSE	MSSIM	FSIM	PSNR	RMSE	MSSIM	FSIM
3	Noisy image	37.83	10.71	0.9068	0.973	37.55	11.43	0.8712	0.97
	Bilateral	40.23	6.17	0.9707	0.9861	40.83	5.37	0.9718	0.9862
	Multi resolution bilateral	35.1	20.1	0.9395	0.9549	37.32	12.06	0.9730	0.9744
	Scaled bilateral	40.2	6.21	0.9794	0.9902	40.44	5.87	0.9854	0.9904
	Non local means	38.42	9.36	0.9853	0.9899	40.18	6.23	0.9906	0.9918
	Proposed method	40.69	5.55	0.979	0.9896	41.56	4.54	0.9845	0.9906
5	Noisy image	33.4	29.75	0.8384	0.9358	33.11	31.74	0.7937	0.93
	Bilateral	35.15	19.86	0.8992	0.9517	35.46	18.48	0.8867	0.949
	Multi resolution bilateral	32.89	33.41	0.9100	0.9334	33.89	26.52	0.9467	0.9538
	Scaled bilateral	35.83	16.98	0.931	0.9667	36.21	15.58	0.9368	0.9658
	Non local means	37.32	12.06	0.9772	0.9840	38.73	8.72	0.9851	0.9871
	Proposed method	36.66	14.02	0.9538	0.9769	37.57	11.38	0.9683	0.9789
7	Noisy image	30.47	58.29	0.7705	0.8942	30.19	62.2	0.7248	0.8838
	Bilateral	31.87	42.27	0.8144	0.9084	32.07	40.39	0.7892	0.9019
	Multi resolution bilateral	30.92	52.67	0.8713	0.9037	31.67	44.27	0.9164	0.9284
	Scaled bilateral	32.64	35.43	0.8551	0.9297	32.99	32.7	0.8521	0.9259
	Non local means	36.12	15.87	0.9672	0.9772	37.37	11.90	0.9780	0.9817
	Proposed method	33.58	28.47	0.9007	0.9523	34.2	24.31	0.9107	0.9508
10	Noisy image	27.38	118.87	0.6733	0.8336	27.1	126.89	0.6332	0.8193
	Bilateral	28.48	92.17	0.6986	0.8439	28.63	89.22	0.67	0.8337
	Multi resolution bilateral	29.09	80.25	0.8233	0.8664	29.81	67.88	0.8781	0.8959
	Scaled bilateral	29.27	76.88	0.7364	0.8686	29.52	72.61	0.7201	0.81
	Non local means	34.36	23.79	0.9489	0.9651	35.52	18.25	0.9644	0.9717
	Proposed method	31.22	49.06	0.8613	0.9349	31.81	42.8	0.8991	0.9418
15	Noisy image	23.87	266.81	0.5358	0.7467	23.58	285.02	0.5089	0.7285
	Bilateral	24.7	220.34	0.545	0.7518	24.83	213.77	0.5239	0.7386
	Multi resolution bilateral	27.07	127.77	0.7577	0.8182	27.71	110.23	0.8202	0.8523
	Scaled bilateral	25.5	183.17	0.5763	0.7775	25.69	175.35	0.5585	0.7641
	Non local means	31.71	43.87	0.9088	0.9380	32.63	35.46	0.9316	0.9477
	Proposed method	26.72	138.47	0.6579	0.8365	27.27	121.91	0.6964	0.8476

```

10.     $\rho(i,j) = \rho_m ;$ 
11.    else
12.       $\rho(i,j) = \rho_l ;$ 
13.    end
14.    else
15.      ifREM(x,y) == 1
16.         $\rho(i,j) = \rho_s ;$ 
17.      else
18.         $\rho(i,j) = \rho_s ;$  (This should not occur)
19.      end
20.    end
21. end

```

The proposed filter is designed as follows

$$\Delta'(i,j) = \rho(i,j)(\psi(i,j)\zeta(i,j)) \quad (8)$$

The first condition (1) emphasizes that whether neighbor pixel is near to an edge or not. The granule processing will give a thick edge which will also consider pixels near to actual edges. Conditions (1) – (6) reveal that the edge may pass through neighbor pixel and both are from same class, so current pixel is also near to an edge hence assign moderate weight to preserve that edge. Otherwise both the pixel belongs to different classes and hence assigns small weight so that it will have less impact.

If an edge is not passing through neighbor pixel then check whether they belong to same class or not in condition (8). If both are from same class and edge is passing from center pixel (condition (9)) then assign moderate weight to preserve that edge, otherwise (condition (11)), they both belong to homogeneous area and have

high dependency on each other so assign high weight to increase the impact.

If both pixel and its neighbor do not belong to same class (condition (14)) and center pixel is an edge pixel (condition (15)) then both belong to different classes and edge is passing in between these two, so assign small weight. The condition (17) should not occur ideally (but this case has been observed in experiments), so assign small weight to have less impact on the current pixel.

3.4. Computational complexity

In this section, we evaluate the computational complexity of the proposed method along with other methods which are used for comparison. All the methods based on Bilateral Filter are window based method, in other words, methods are restricted in sufficient large window around current pixel for estimating its true value. Let S be the predefined size of the neighborhood such as $3 \times 3, 5 \times 5$ etc. and N be the total number pixel of the image. Here, we assume that S involves in the computation of spatial and range filters as defined in Section 2. Being a point-wise processing method, for each pixel computation of both filters need to be performed. Hence the complexity of Bilateral Filter [7] can be defined as $O(NS)$ [22]. In extreme case (worst case complexity), S can be extended to image space which makes complexity in order of $O(N^2)$.

In case of Scaled Bilateral Filter [10], first scaled version of input image is computed using Gaussian function with filter size K and range filter is based on difference between scaled image and input image for each pixel. Hence, the complexity can be defined as $O(N(S+K))$. The Multi-Resolution Bilateral Filter [13] is based only Bilateral Filter with additional two level wavelet decomposition.

Table 5

Performance comparison of proposed denoising filter with other approaches on various quantitative measures under **Rician Noise** assumption on **T2** images of Brain Web database.

Noise SD	Methods	Slice 70				Slice 100			
		PSNR	RMSE	MSSIM	FSIM	PSNR	RMSE	MSSIM	FSIM
3	Noisy image	37.83	10.71	0.9123	0.9773	37.55	11.42	0.8787	0.9741
	Bilateral	40.17	6.25	0.972	0.9881	40.81	5.4	0.9738	0.9885
	Multi resolution bilateral	30.74	54.88	0.8868	0.9099	32.80	34.10	0.9468	0.9458
	Scaled bilateral	39.17	7.88	0.9801	0.9913	38.79	8.6	0.9868	0.9923
	Non local means	34.00	25.86	0.9834	0.9871	34.85	21.27	0.9983	0.9886
	Proposed method	40.6	5.66	0.98	0.9909	41.48	4.62	0.9861	0.9924
7	Noisy image	30.5	58	0.7834	0.9128	30.21	61.93	0.7412	0.9005
	Bilateral	31.88	42.22	0.8238	0.9241	32.06	40.47	0.8006	0.9159
	Multi resolution bilateral	27.99	103.18	0.8430	0.8754	29.23	77.61	0.9044	0.9110
	Scaled bilateral	32.54	36.21	0.866	0.9442	32.76	34.43	0.8653	0.9422
	Non local means	32.61	35.69	0.9652	0.9738	33.45	29.38	0.9770	0.9785
	Proposed method	33.21	31.07	0.8953	0.956	34.07	25.46	0.9161	0.959
10	Noisy image	27.42	117.88	0.6959	0.8644	27.13	126.03	0.6592	0.8642
	Bilateral	28.54	90.98	0.718	0.8725	28.65	88.74	0.6901	0.8578
	Multi resolution bilateral	26.28	153.24	0.8120	0.8522	27.14	125.76	0.8710	0.8838
	Scaled bilateral	29.29	76.53	0.757	0.896	29.5	73.08	0.7429	0.8865
	Non local means	31.49	46.08	0.9476	0.9622	32.33	38.03	0.9643	0.9681
	Proposed method	31.2	49.36	0.8921	0.9312	31.26	48.66	0.893	0.9434
15	Noisy image	23.92	263.54	0.5782	0.7965	23.63	282.14	0.554	0.7722
	Bilateral	24.79	215.91	0.5849	0.8002	24.85	212.87	0.564	0.779
	Multi resolution bilateral	23.98	260.19	0.7603	0.8139	24.65	222.93	0.8209	0.8404
	Scaled bilateral	25.57	180.15	0.6144	0.8222	25.71	174.51	0.5969	0.8043
	Non local means	29.63	70.73	0.9095	0.9401	30.42	59.01	0.9355	0.9485
	Proposed method	28.3	96.19	0.7884	0.8987	28.52	91.39	0.7914	0.8946
20	Noisy image	21.46	465	0.4908	0.7428	21.16	498.27	0.4763	0.7151
	Bilateral	22.03	407.82	0.4875	0.7406	22.05	405.47	0.4742	0.716
	Multi resolution bilateral	22.20	392.16	0.7092	0.7733	22.68	350.48	0.7705	0.7944
	Scaled bilateral	22.92	331.81	0.5141	0.7625	23.0	326.71	0.5	0.7391
	Non local means	27.84	107.00	0.8655	0.9178	28.68	8.11	0.9005	0.9285
	Proposed method	24.76	217.34	0.6114	0.8253	24.67	222.03	0.5865	0.8056
25	Noisy image	19.56	720.13	0.4248	0.6987	19.26	771.56	0.4168	0.6697
	Bilateral	19.77	684.97	0.4133	0.6896	19.79	682.89	0.4061	0.6634
	Multi resolution bilateral	20.99	517.51	0.6712	0.7411	21.14	500.2480	0.7230	0.7513
	Scaled bilateral	20.77	544.15	0.4378	0.7117	20.8	540.85	0.4281	0.6855
	Non local means	26.22	155.42	0.8216	0.8963	27.06	127.92	0.8627	0.9073
	Proposed method	21.49	461.31	0.4746	0.7493	21.36	474.92	0.4585	0.7211

The method deploy three times Bilateral Filter at various stages (Refer to schema provided in [13]). Hence, computationally it can be defined in terms of $O(3NS + W)$, where W denotes the computation required for two level decomposition and reconstruction.

The proposed method first computes Class information and Edge information based on three optimized thresholds (see Sections 3.1 and 3.2). Note that, in the current context, as we know there are four classes possible, hence the number of thresholds is fixed to three. Let us consider, T_{avg} number of intensity values are considered to find each optimized threshold. So the complexity of this task would be $O(N * T_{avg})$. Now while designing the filter, an additional step is proposed along with the conventional Bilateral Filter. This additional step assigns weight to each pixel by comparing class information and edge information. Hence, the overall computational complexity becomes $O(N(S+C) + N * T_{avg})$, where C denotes the time to compute weights. In extreme case, if S and C are extended to image space, then complexity turns out to be $O(N^2)$ which is same as Bilateral Filter. Thus, it could be concluded that the proposed method does not carry high computational cost.

4. Experimental results

The work has been carried out on 2D monochrome human brain MR images. The experiments are performed on one simulated

dataset downloaded from Brain Web [38] and two real data sets, Open Access Series of Imaging Studies (OASIS, [39]) and Brain Tumor Segmentation challenge data from MICCAI 2012 conference (BRATS, [40]). The experiment setup considers two noise models, Gaussian and Rician in nature on Brain Web data. The method of addition of rician noise is same as that presented in [27]. To evaluate performance of denoising algorithm, four evaluation measures are used. The measures are of Peak Signal to Noise Ratio (PSNR), Root Mean Square Error (RMSE), Structure SIMilarity (SSIM) Index proposed in [23] and Feature SIMilarity (FSIM) Index proposed in [24]. Note that these performance measures are widely used to validate denoising algorithms. In the real databases, noise is assumed to be Rician in nature. The parameters of all methods are mentioned in the Table 1. All the experiments are performed in MATLAB 2012(b) environment on Lenovo Z580 with Intel core i7 Windows7 laptop. The next section briefly describe the evaluation measure in more detail followed by experimental set up and results on all the data sets.

4.1. Evaluation measures

The evaluation measures used are defined as follows: Let I be noise-free image of size $M \times N$ and (\hat{I}) be its noise-free approximation.

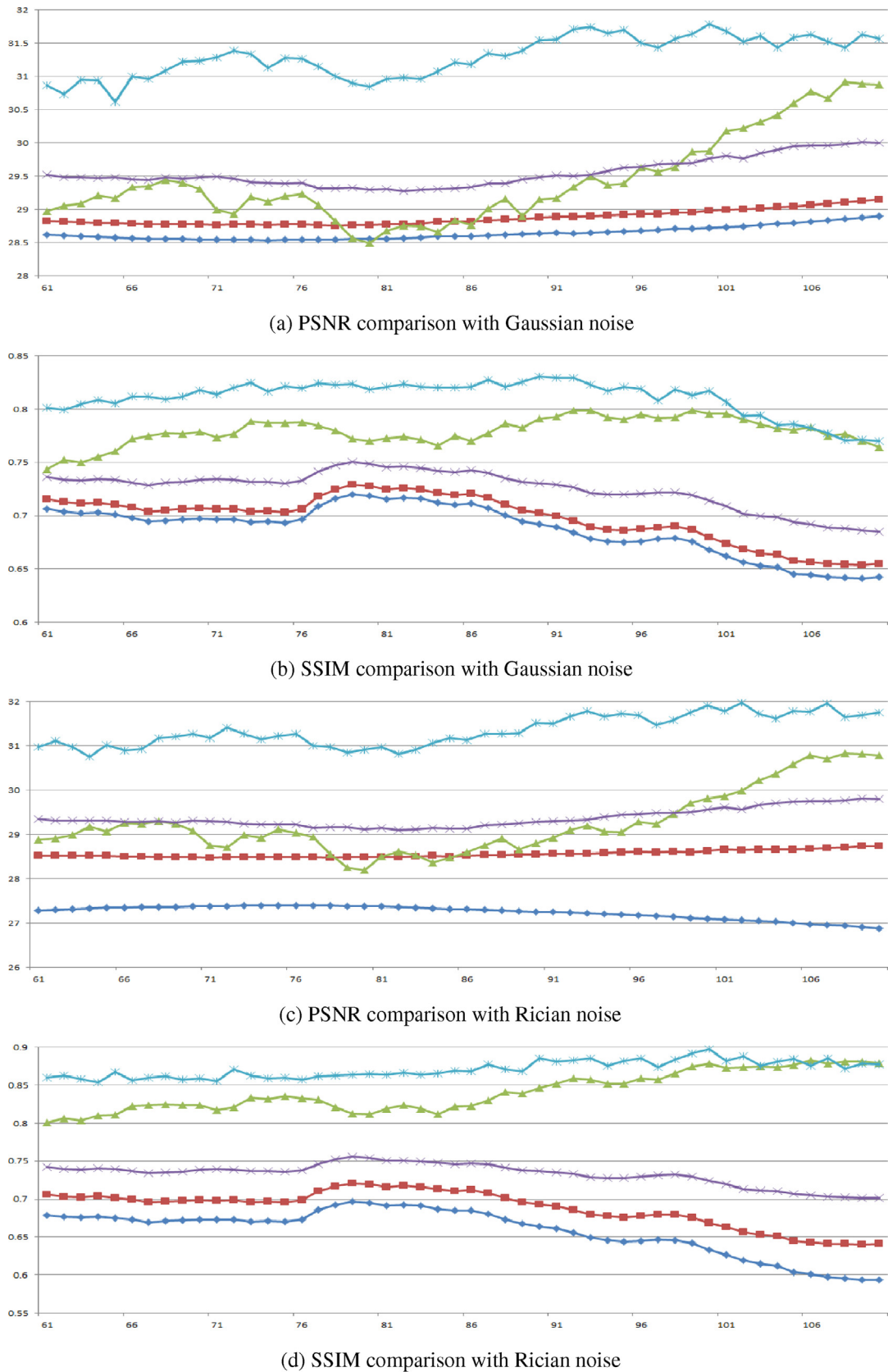


Fig. 4. Graphs for PSNR & SSIM comparison of T1 images with Gaussian noise in (a) and (b) and with Rician noise in (c) and (d) respectively with noise level 10. The y-axis represents PSNR values in dB in graphs (a) and (c) and SSIM values in range [0,1] in graphs (b) and (d) where as x-axis represents 50 slices of the T1 data indexed from 61 to 110.

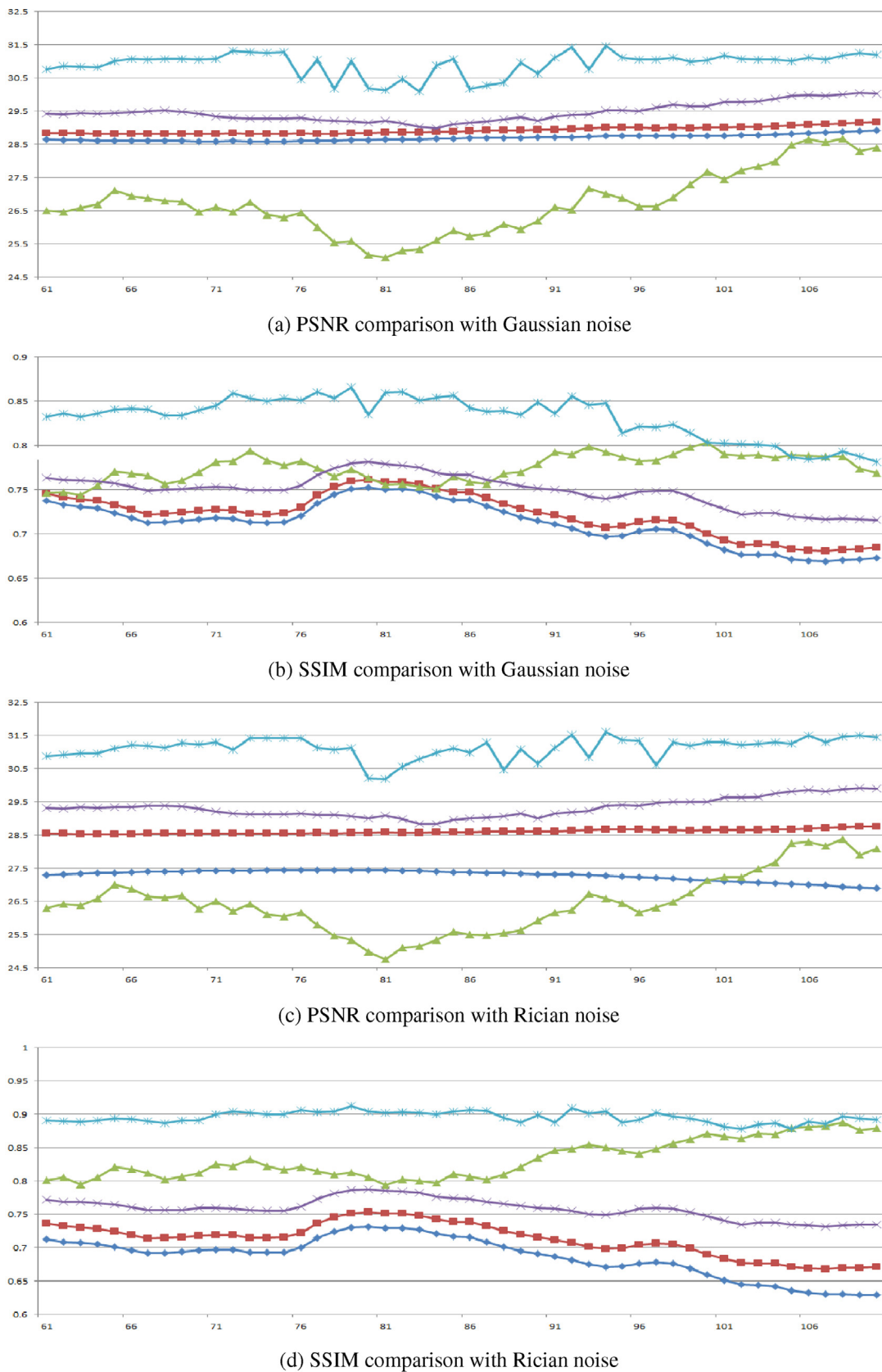


Fig. 5. Graphs for PSNR & SSIM comparison of T2 images with Gaussian noise in (a) and (b) and with Rician noise in (c) and (d) respectively with noise level 10. The y-axis represents PSNR values in dB in graphs (a) and (c) and SSIM values in range [0,1] in graphs (b) and (d) where as x-axis represents 50 slices of the T2 data indexed from 61 to 110.

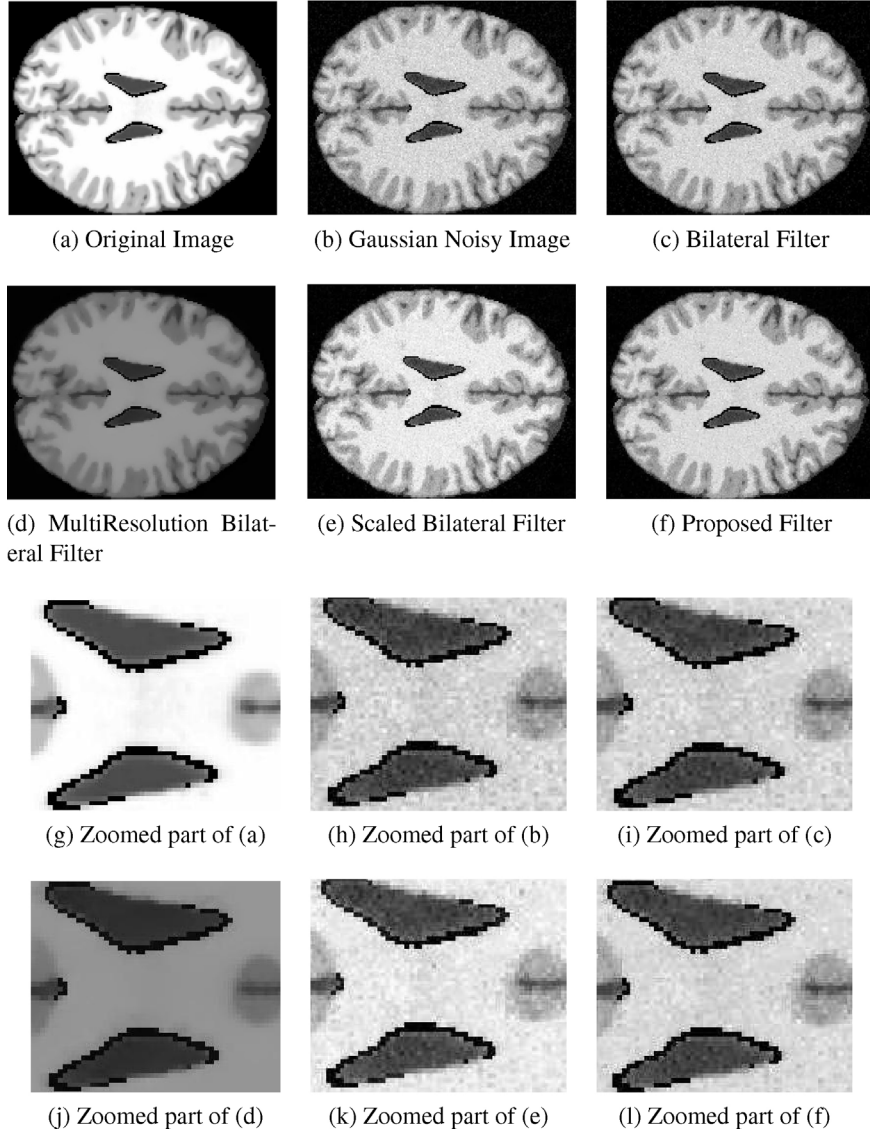


Fig. 6. Results on brain web data (slice 100) having Gaussian noise with zero mean and standard deviation 5.

- Root Mean Square Ratio (RMSE)

$$\text{MeanSquareError}(MSE) = \frac{1}{MN} \sum_{i=1}^M \sum_{j=1}^N (I(i,j) - \hat{I}(i,j))^2$$

$$RMSE = \sqrt{MSE} \quad (9)$$

- Peak-Signal-to-Noise Ratio (PSNR)

$$PSNR = 10\log_{10} \left(\frac{L^2}{MSE} \right) \quad (10)$$

where L is maximum intensity level present in the image I and MSE is same as defined above.

- Structural Similarity Index (SSIM) [23]

$$SSIM(x, y) = \frac{(2\mu_x\mu_y + \epsilon_1)(2\sigma_{xy} + \epsilon_2)}{(\mu_x^2 + \mu_y^2 + \epsilon_1)(\sigma_x^2 + \sigma_y^2 + \epsilon_2)}$$

$$MSSIM = \frac{1}{M} \sum_{j=1}^M SSIM(x_j, y_j) \quad (11)$$

where ϵ_1, ϵ_2 ensure stability when either $(\mu_x^2 + \mu_y^2)$ or $(\sigma_x^2 + \sigma_y^2)$ is close to zero. The SSIM is defined over a local window centered at (x, y) and average over such windows gives a single measure for entire image, named as Mean SSIM (MSSIM).

- Feature Similarity Index (FSIM) [24]

$$FSIM = \frac{\sum_{x \in \Omega} S_L(x) PC_m(x)}{\sum_{x \in \Omega} PC_m(x)} \quad (12)$$

where Ω defines entire image spatial domain. The similarity measure $S_L(x)$ is defined as product of similarity function on Phase Congruency (PC) and similarity function of Gradient Magnitude (GM) (i.e. $S_L(x) = S_{PC}(x) \cdot S_G(x)$). The functions $S_{PC}(x)$ and $S_G(x)$ are as follows:

$$S_{PC}(x) = \frac{2PC_1(x).PC_2(x) + \epsilon_1}{PC_1^2(x) + PC_2^2(x) + \epsilon_1} \quad \& S_G(x) = \frac{2G_1(x).G_2(x) + \epsilon_2}{G_1^2(x) + G_2^2(x) + \epsilon_2} \quad (13)$$

where ϵ_1, ϵ_2 ensure stability of above functions.

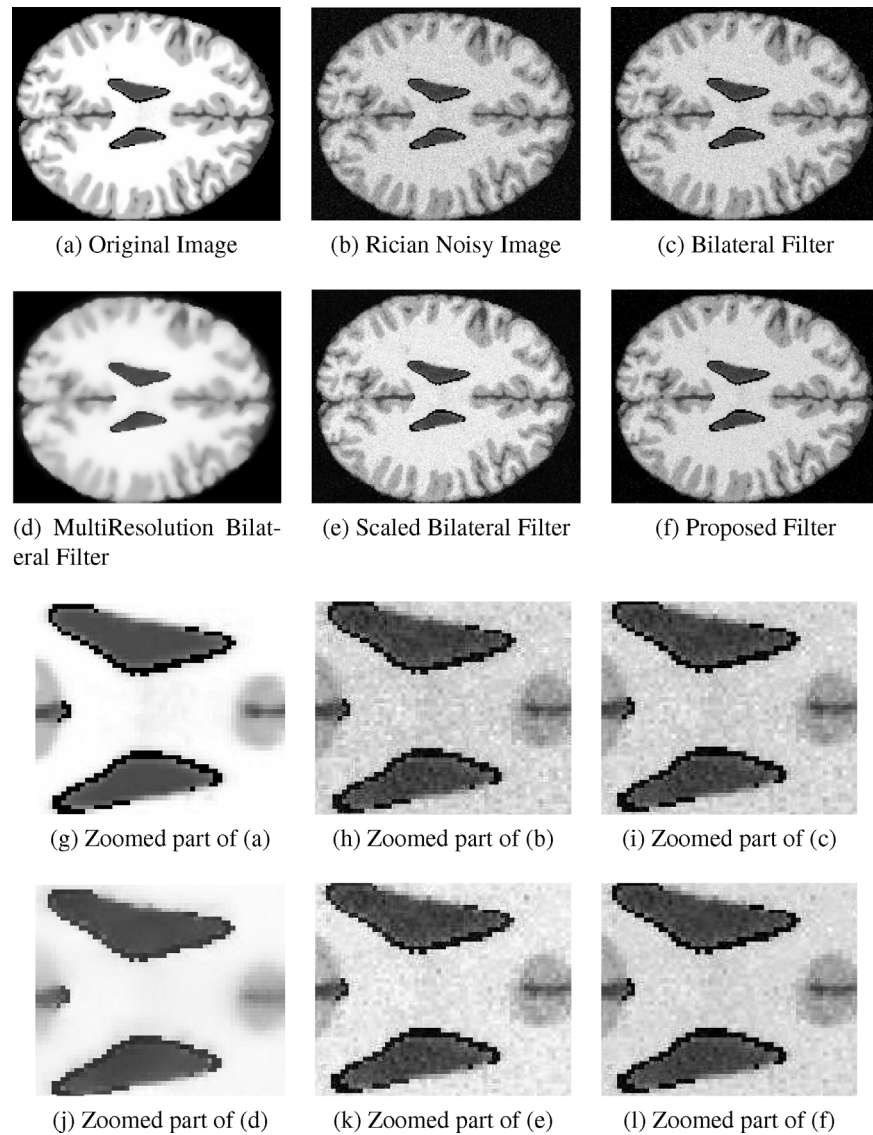


Fig. 7. Results on brain web data (slice 100) having Rician noise with zero mean and standard deviation 10.

4.2. Simulation results

4.2.1. Results on brain web database

The implementation of algorithm on phantom data provides an insight of the algorithm and ability to compare the results with available ground truth data. The Brain Web database [38] consists of phantom volumetric data with their ground truth details. The other specifications of database are: size = $181 \times 217 \times 181$, modality = T_1 & T_2 , protocol = ICBM, RF=0% and noise = 0%. The 2D slices are extracted from 3D volume data of size 140×176 after removing unnecessary background area and normalized in the range [0, 1] (Fig. 3).

The experiments are performed with different noise levels by adding Gaussian noise and Rician noise in the data. The addition of noise is done as suggested in [27]. In case of Rician noise, the bias removal ($= 2\sigma^2$, where σ is noise standard deviation) is also done as suggested in [26]. The results of both noise models with different noise levels are shown in Tables. Tables 2 and 3 show results on Gaussian noise distribution over T1 and T2 images. In most of the cases, proposed method clearly outperforms than other methods. Tables 4 and 5 show results on Rician noise distribution over both the modalities. In all the cases, NLM filter clearly outperforms

from class of Bilateral Filters. However, proposed method is performed better than other methods of filters in Bilateral category. The experiments were performed on 50 slices of both the modalities on Gaussian noise and Rician noise with noise level 10. The results of PSNR and SSIM values are shown in Figs. 4 and 5 where one can observe the superior performance among Bilateral Filters (Note, we have shown results on Bilateral class of filters only). The Figs. 6 and 7 show the denoised images with various methods on slice 100 of T1 modality under Gaussian noise and Rician noise respectively.

4.2.2. Results on real database

The other two real datasets are having some pathological issues. The subject details of selected data from OASIS dataset [39] are as follows: Subject ID:0018, Age: 39 (male), scan number: mpr-1, type: MPRAGE, voxel resolution: $1.0 \text{ mm} \times 1.0 \text{ mm} \times 1.25 \text{ mm}$, Orientation: Sagittal, TR (ms)=9.7, TE (ms)=4.0, TI(ms)=20.0, Flip angle=10, slice number used = 100. The results are shown in Fig. 8 along with their zoomed in portion for more clarity.

Another dataset is selected from BRATS data [40] where actual challenge was to identify tumor region and other pathological disorder. The details of the subjects are as follows: Subject ID: 0015, having high grade gliomas, slice= 100. In the real datasets, the noise

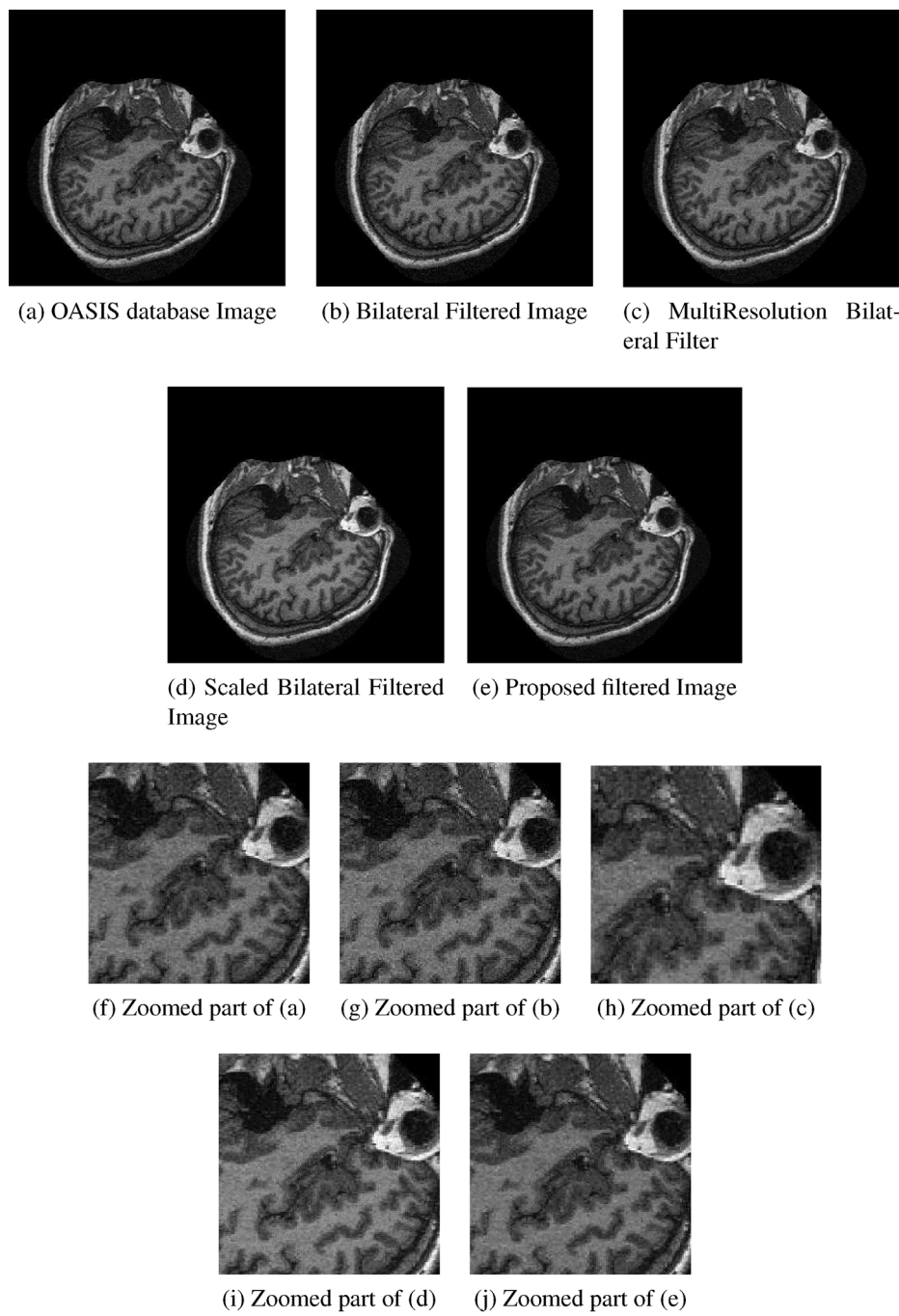


Fig. 8. Result on MR slice from OASIS database.

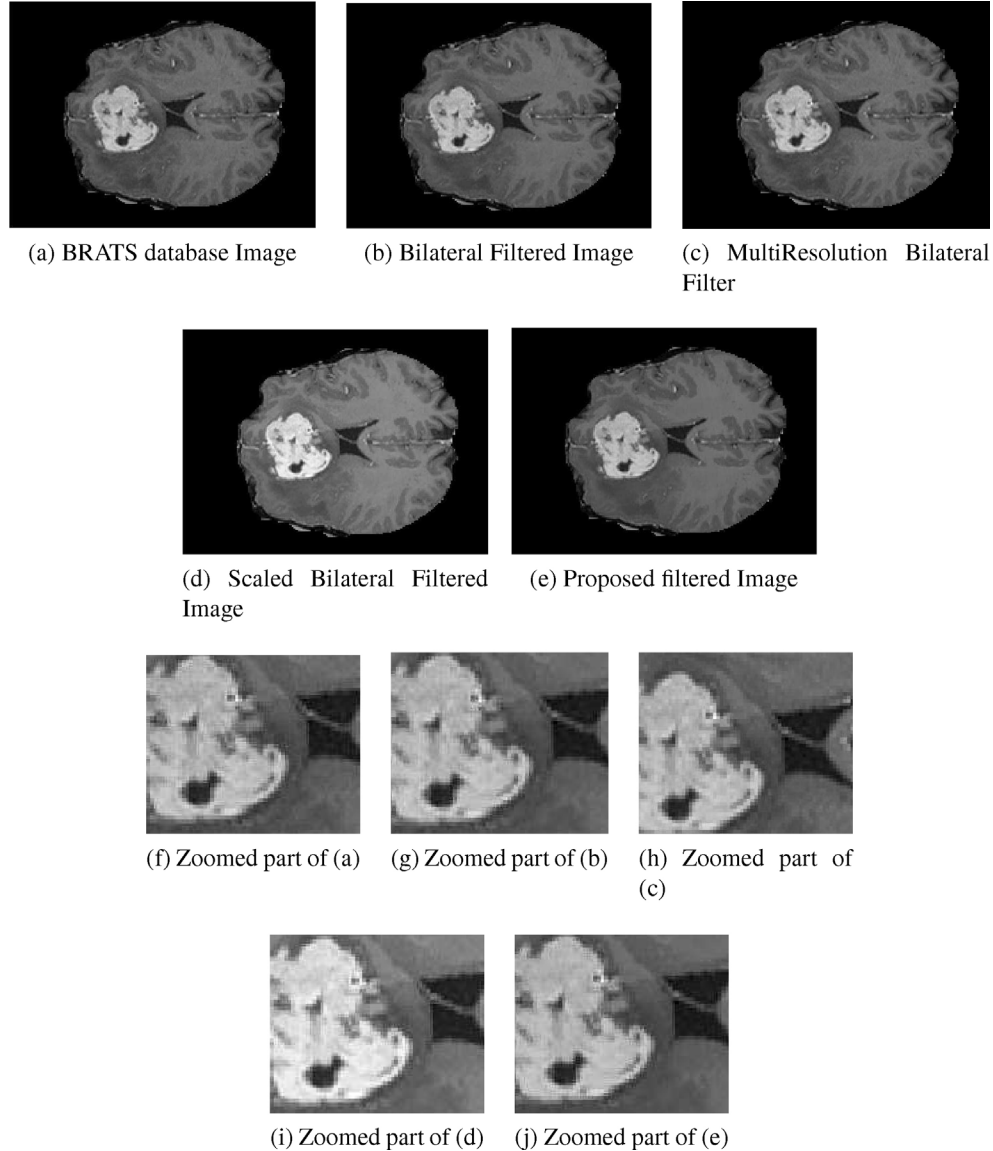


Fig. 9. Result on MR slice from MICCAI BRATS 2012 database.

model was assumed to Rician in nature [1]. The rician noise estimation was done using recently proposed method in [41]. The results are shown in Fig. 9. The Fig. 10 shows the estimated Tumor class in comparison with the ground truth provided by the organizers. The

Dice coefficient is found to be 0.71 where labels are re-estimated using approach of Section 3.1 after denoising.

5. Conclusion

Rough set has capacity to handle the uncertainty present in the data. This characteristic of RST enables it to suitable candidate to obtain Edge and Class information form the noisy image. The edge information and class information in-turn boost up the performance of the proposed filter. The obtained edge map is found to be continuous and closed and is capable of defining object boundaries even in noisy situations. It appeared to be defining object boundaries in a better way compared to a couple of existing methodologies such as Canny Edge Detector, Active Contour methods. The performance of the proposed filter, hence found to be satisfactory when compared with the existing Bilateral Filters. Note that the performance of present filter for denoising is not compared with some of the recent techniques included within paradigm of

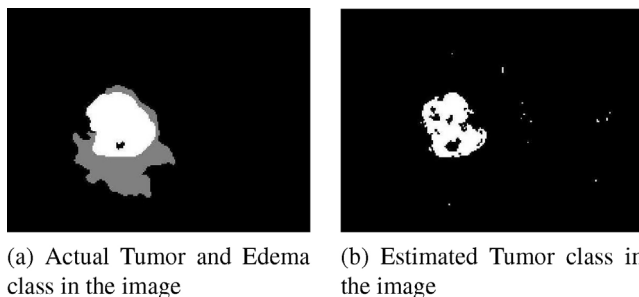


Fig. 10. The comparison of actual class and estimated using rough class labels is shown where Dice coefficient is found to be 0.71.

non-local means. These methodologies are based on very different principle and hence not compared.

References

- [1] H. Gudbjartsson, S. Patz, The Rician distribution of noisy MRI data, *Magnet. Reson. Med.* 34 (6) (1995) 910–914.
- [2] P. Perona, J. Malik, Scale space and edge detection using anisotropic diffusion, *IEEE Trans. Pattern Anal. Mach. Intell.* 12 (7) (1990 July) 629–639.
- [3] G. Gerig, O. Kubler, R. Kikinis, F.A. Jolesz, Nonlinear anisotropic filtering of MRI data, *IEEE Trans. Med. Imaging* 11 (2) (1992) 221–232.
- [4] J. Weickert, Anisotropic diffusion in image processing, vol. 1, Teubner Stuttgart, 1998.
- [5] M.J. Black, G. Sapiro, D.H. Marimont, D. Heeger, Robust anisotropic diffusion, *IEEE Trans. Image Process.* 7 (3) (1998) 421–432.
- [6] V.B. Surya Prasath, A. Singh, Edge detectors based anisotropic diffusion for enhancement of digital images, in: Sixth Indian Conference on Computer Vision, Graphics & Image Processing, ICVGIP'08, IEEE, 2008, pp. 33–38.
- [7] C. Tomasi, R. Manduchi, Bilateral filtering for gray and color images, in: IEEE International Conference on Computer Vision, 1998, pp. 9–846.
- [8] M. Elad, On the origin of the bilateral filter and ways to improve it, *IEEE Trans. Image Process.* 11 (10) (2002) 1141–1151.
- [9] G. Sicuranza, Nonlinear Image Processing, Access Online via Elsevier, 2000.
- [10] S.M. Aswatha, J. Mukhopadhyay, P. Bhawmick, Image denoising by scaled bilateral filtering, in: Third National Conference on Computer Vision, Pattern Recognition, Image Processing and Graphics (NCVPRIPG), IEEE, 2011, pp. 122–125.
- [11] S. Paris, F. Durand, A fast approximation of the bilateral filter using a signal processing approach, in: Computer Vision-ECCV 2006, Springer, 2006, pp. 568–580.
- [12] Y. Zhang, X. Tian, P. Ren, An adaptive bilateral filter based framework for image denoising, *Neurocomputing* 140 (2014) 299–316.
- [13] M. Zhang, B.K. Gunturk, Multiresolution bilateral filtering for image denoising, *IEEE Trans. Image Process.* 17 (12) (2008) 2324–2333.
- [14] F. Porikli, Constant time o(1) bilateral filtering, in: IEEE Conference on Computer Vision and Pattern Recognition, 2008. CVPR 2008, IEEE, 2008, pp. 1–8.
- [15] Q. Yang, N. Ahuja, Kar-Han Tan, Constant time median and bilateral filtering, *Int. J. Comput. Vis.* (2014) 1–12.
- [16] W.C.K. Wong, A.C.S. Chung, S.C.H. Yu, Trilateral filtering for biomedical images, in: IEEE International Symposium on Biomedical Imaging: Nano to Macro, 2004, IEEE, 2004, pp. 820–823.
- [17] R. Garnett, T. Huegerich, C. Chui, W. He, A universal noise removal algorithm with an impulse detector, *IEEE Trans. Image Process.* 14 (11) (2005) 1747–1754.
- [18] J. Canny, A computational approach to edge detection, *IEEE Trans. Pattern Anal. Mach. Intell.* 8 (6) (1986) 679–698.
- [19] M. Kass, A. Witkin, D. Terzopoulos, Snakes: active contour models, *Int. J. Comput. Vis.* 1 (4) (1988) 321–331.
- [20] T.F. Chan, L.A. Vese, Active contours without edges, *IEEE Trans. Image Process.* 10 (2) (2001) 266–277.
- [21] Z. Pawlak, Rough sets, *Int. J. Comput. Inform. Sci.* 11 (5) (1982) 341–356.
- [22] S. Paris, P. Kornprobst, J. Tumblin, F. Durand, Bilateral filtering: theory and applications, *Found. Trends® Comput. Graph. Vis.* 4 (1) (2008) 1–73.
- [23] Z. Wang, A.C. Bovik, H.R. Sheikh, E.P. Simoncelli, Image quality assessment: from error visibility to structural similarity, *IEEE Trans. Image Process.* 13 (4) (2004 April) 600–612.
- [24] L. Zhang, L. Zhang, X. Mou, D. Zhang, Fsim: A feature similarity index for image quality assessment, *IEEE Trans. Image Process.* 20 (9) (2011 Sept) 2378–2386.
- [25] A. Buades, B. Coll, J.M. Morel, A non local algorithm for image denoising, *IEEE Comput. Vis. Pattern Recognit.* 6 (2005) 0–65.
- [26] J.V. Manjón, J.C. Caballero, G.G. Martí, L. Martí-Baonmati, M. Robles, MRI denoising using non local means, *Med. Image Anal.* 12 (2008) 514–523.
- [27] P. Coupe, P. Yger, S. Prima, P. Hellier, C. Kervrann, C. Barillot, An optimized blockwise nonlocal means denoising filter for 3d magnetic resonance images, *IEEE Trans. Med. Imaging* 27 (4) (2008 April) 425–441.
- [28] J. Manjón, P. Coupé, A. Buades, D. Louis Collins, M. Robles, New methods for MRI denoising based on sparseness and self-similarity, *Med. Image Anal.* 16 (1) (2012) 18–27.
- [29] K. Dabov, A. Foi, V. Katkovnik, K. Egiazarian, Image denoising by sparse 3d transform domain collaborative filtering, *IEEE Trans. Image Process.* 16 (8) (2007 August) 2080–2095.
- [30] L. Zhang, W. Dong, D. Zhang, G. Shi, Two-stage image denoising by principal component analysis with local pixel grouping, *Pattern Recogn.* 43 (4) (2010 April) 1531–1549.
- [31] M. Aharon, M. Elad, A. Bruckstein, K-svd: an algorithm for designing overcomplete dictionaries for sparse representation, *IEEE Trans. Signal Process.* 54 (11) (2006) 4311–4322.
- [32] A. Rajwade, A. Rangarajan, A. Banerjee, Image denoising using the higher singular value decomposition, *IEEE Trans. Pattern Anal. Mach. Intell.* 35 (4) (2013 April) 849–862.
- [33] A. Phophalia, A. Rajwade, S.K. Mitra, Rough set based image denoising for brain MR images, *Signal Process.* 103 (2014) 24–35.
- [34] A. Phophalia, S.K. Mitra, A. Rajwade, A new denoising filter for brain mr images., in: Eighth Indian Conference on Computer Vision, Graphics and Image Processing (ICVGIP), 2012.
- [35] S.K. Pal, B. Uma Shankar, P. Mitra, Granular computing, rough entropy and object recognition, *Pattern Recogn. Lett.* 26 (2005) 2509–2517.
- [36] S. Ashish Phophalia, K. Mitra, A. Rajwade, Object boundary detection using rough set theory, in: Fourth National Conference on Computer Vision, Pattern Recognition, Image Processing and Graphics (NCVPRIPG), 2013.
- [37] L.A. Vese, T.F. Chan, A multiphase level set framework for image segmentation using the Mumford and Shah model, *Int. J. Comput. Vis.* 50 (3) (2002) 271–293.
- [38] D.L. Collins, A. Zijdenbos, V. Kollokian, J. Sled, N. Kabani, C. Holmes, A. Evans, Design and construction of a realistic digital brain phantom, *IEEE Trans. Med. Imaging* 17 (3) (1998 June) 463–468.
- [39] D.S. Marcus, T.H. Wang, J. Parker, J.G. Csernansky, J.C. Morris, R.L. Buckner, Open access series of imaging studies (oasis): cross-sectional MRI data in young middle aged nondemented and demented older adults, *J. Cogn. Neurosci.* 19 (9) (2007) 1498–1507.
- [40] B. Menze, A. Jakab, S. Bauer, M. Reyes, M. Prastawa, K.V. Leemput, Multimodal brain tumor segmentation challenge., in: MICCAI Conference, October, 2012.
- [41] A. Foi, Noise estimation and removal in MR imaging: The variance-stabilization approach, in: ISBI, 2011, pp. 1809–1814.